Cynomolgus and Rhesus Monkey Visual Pigments

Application of Fourier Transform Smoothing and Statistical Techniques to the Determination of Spectral Parameters

FERENC I. HÁROSI

From the Laboratory of Sensory Physiology, Marine Biological Laboratory, Woods Hole, Massachusetts 02543, and the Department of Physiology, Boston University School of Medicine, Boston, Massachusetts 02118

ABSTRACT   Microspectrophotometric measurements were performed on 217 photoreceptors from cynomolgus, *Macaca fascicularis*, and rhesus, *M. mulatta*, monkeys. The distributions of cell types, for rods and blue, green, and red cones were: 52, 12, 47, and 44, respectively, for the cynomolgus, and 22, 4, 13, and 13 for the rhesus. Visual cells were obtained fresh (unfixed), mounted in various media (some containing 11-*cis*-retinal), and then located visually under dim red (650 nm) illumination. Absolute absorbance (A), linear dichroism (LD), and bleaching difference (BD) absorbance spectra were recorded through the sides of outer segments. The spectra were subjected to rigorous selection criteria, followed by digital averaging and Fourier transform filtering. Statistical methods were also applied to the accepted samples in the estimation of population means and variances. The wavelength of mean peak absorbance (λ_{max}) and the standard error at 95% certainty of the rod and blue, green, and red cone pigments in cynomolgus were 499.7 ± 2.5, 431.4 ± 4.2, 533.9 ± 2.4, and 565.9 ± 2.8 nm, respectively. The rhesus pigments were statistically indistinguishable from the cynomolgus, having λ_{max} of ~500, 431, 534, and 566 nm. Statistical tests did not reveal the presence of a λ_{max} subpopulation (i.e., anomalous pigments). The bandwidth of each α-band was determined in two segments, giving rise to the longwave half-density (LWHDBW), shortwave half-density (SWHDBW), and total half-density (THDBW) bandwidths. The LWHDBW was found to have the smallest variance. Both the LWHDBW and the THDBW showed linear dependence on the peak wavenumber $(\lambda_{max})^{-1}$ for the four macaque pigments.

INTRODUCTION

This article is derived from microspectrophotometric experiments carried out during a three-year period ending in April, 1983. Although the initial phase of this work provided material for an earlier presentation (Hárosi, 1982a) and three

records published by MacNichol et al. (1983), a comprehensive analysis of the data has been prompted by the development of a new method for digital smoothing of spectra, a method based on the Fourier transformation. (A similar method was developed independently by MacNichol, 1986.)

Primate visual pigments were first optically characterized by the use of the microspectrophotometric technique over two decades ago. Marks et al. (1964) and Brown and Wald (1964) established the existence of four spectrally distinct substances: three in cone outer segments and one in those of rods (see also MacNichol, 1964). These and other early investigations (e.g., Dobelle et al., 1969) demonstrated the feasibility of the technique and provided approximate values for the visual pigment peak absorbances (λ_{max}). A second flurry of activity provided much more accurate λ_{max} values and, moreover, made inroads into the questions of in situ pigment concentration and α-band spectral bandwidth in primate visual pigments (Bowmaker et al., 1978, 1980, 1983; Dartnall et al., 1983a, b; MacNichol et al., 1983; Mansfield et al., 1984; Levine and MacNichol, 1985; Mansfield, 1985). Nevertheless, uncertainties prevail in the specific pigment density of primate photoreceptors, in the bandwidth of their absorbance spectra, and even in the λ_{max} values, especially for those of the blue-absorbing cones.

Work in this field has been hampered by the scarcity and expense of the tissue and our inability to curb in vitro cellular deterioration. The largely unrecognized risk of exposure to infectious agents while experimenting with such material should also be mentioned as a source of difficulty.

The dichroic microspectrophotometer (DMSP) was used throughout (Hárosi and MacNichol, 1974b). Recent modifications of the DMSP (Hárosi, 1982a, b) resulted in increased sensitivity for the detection of anisotropic absorbance; this feature turned out to be advantageous because the rapid and extensive postmortem deterioration of monkey visual cells usually leads to the loss of all but the faintest linear dichroism. The combined use of absolute absorbance (A), bleaching difference absorbance (BD), and linear dichroism (LD) spectra permitted a more confident delineation of λ_{max} values than could be achieved from absorbance spectra alone. In an effort to retard cell breakdown in vitro, several suspending media were tried; their compositions occasionally included the addition of vitamins E and C. Exogenous 11-cis-retinal (the aldehyde of vitamin A₁) was also used in some cell suspensions for a twofold purpose: to prevent cell deterioration and to provide a source of free chromophore for visual pigment regeneration. Although there was no intentional exposure to visible light of either the eyes or their tissue fragments, the incubation with 11-cis-retinal allowed regeneration to take place among the inadvertently bleached molecules. Beyond the use of these refinements in experimental techniques, the application of digital Fourier transform smoothing to the recorded spectra and statistical analyses to the spectral parameters are described in this contribution.

METHODS

Experimental Animals

The eye tissue used in this study was derived from a total of 28 monkeys: 19 cynomolgus (*Macaca fascicularis*) and 9 rhesus (*M. mulatta*). The majority of the eyes (from 23 animals)

were purchased from Flow Laboratories, Inc., McLean, VA. The eyes of two animals were donated by the New England Regional Primate Research Center, Southborough, MA, while three live monkeys were obtained by R. J. W. Mansfield at Harvard University. More than half the animals were 2–3.5 yr of age; the rest were between 1.5 and 7 yr. Among the cynomolgus monkeys, there were eight males, six females, and five of unknown sex. In the rhesus group, five were identified as males, two as females, and two were unidentified. The retinal tissue from most of these animals was shared among the group comprised of Drs. E. F. MacNichol, Jr., R. J. W. Mansfield, J. S. Levine, and the author.

Anesthetized animals were enucleated under deep red light, usually between 5 and 6 a.m. The eyes were first placed in ice water, then wrapped in aluminum foil, packed with ice in styrofoam containers, and shipped from Washington by air. Experiments normally commenced ~6 h postmortem. This delay was reduced to 1–4 h with animals obtained locally. Experimentation usually continued for a period of 6–12 h, or as long as photoreceptors could be found; occasionally it even continued to the second day.

Safety Precautions

During the earlier part of this project, we treated primate eye tissues as if they were frog or fish. This was a serious mistake, for the macaques are known to be carriers of not only bacterial agents such as tuberculosis, but also viruses pathogenic to humans. Thanks to Dr. John L. Sever of The National Institute of Neurological and Communicative Disorders and Stroke, we learned that exposure to simian B virus must be reckoned with while working with such materials. As of August, 1982, there had been seven cases of simian B infection in humans, causing six fatalities and one hopelessly grave condition. In Dr. Sever's experience at the NIH, 2 out of 4,000 monkeys were found to have active infection of the simian B type. Therefore, although the danger is small, it is nevertheless real. The prudent countermeasures he suggested were as follows. (*a*) The use of disposable masks, gowns, gloves, plastic dishes, and diapers with impermeable lining to contain spills. (*b*) The use of a virologists' hood, or a bacteriologists' "dead-box," in which to carry out gross dissections. Ideally, this should also be equipped with an ultraviolet light source to disinfect the inside surfaces when not in use. (*c*) The disposal of all tissue by submerging in, and the disinfection of exposed instruments and surfaces with, Clorox (sodium hypochlorite, The Clorox Co., Oakland, CA). We adopted these precautionary measures (in collaboration with Drs. E. F. MacNichol, Jr., R. J. W. Mansfield, and J. S. Levine) and believe them to be effective for handling human as well as all nonhuman primate eye tissues.

Preparation

Gross dissection of the eyes was carried out under dim red light, and under sterile conditions, at least for the latter part of the project (see above). With the aid of an infrared dissecting microscope, the retina was removed from the eyecup while submerged in saline solution, and then usually bisected with scissors through the optic disk and fovea so that the available tissue could be shared. The location of the fovea under infrared light could often be visualized as a split in the retina caused by its extreme thinness and weakness there. Central, near-foveal retinal tissue was used preferentially. Areas of ~1 mm² were cut at a time, placed on a no. 1½ coverslip, and teased apart with sharp forceps in a small drop of the final bathing solution. This was covered carefully with a second no. 1½ coverslip of somewhat smaller size, blotted gently along the edges, and sealed in the usual manner (cf. Hárosi and MacNichol, 1974a).

Saline Solutions

The general intent in choosing the composition of bathing media for primate retinal tissue was not only to reproduce the in vivo environment to the best of our ability, but

also to supplement the milieu with agents that might be beneficial in curbing cell deterioration in vitro. The osmotic activity and pH were usually in the ranges of 300–350 mosmol/kg and 7.3–7.5, respectively. A summary of the constituents for the bathing media is shown in Table I. The solution designated B_0 was used most frequently. In a few experiments, the listed solutions were modified. For example, glucose was replaced by 2-deoxy-d-glucose in B_0; in B_4, 0.1 mM diamox was added. Several other combinations of these substances, as well as various proportions, were also tried. Some of the media, although by no means all, were also supplemented with 11-cis-retinal. The usual procedure was to make up one of the solutions freshly from stock solutions just before an experiment. A certain portion of it was used for dissection; the rest was used to mount "control" preparations or to serve as a medium for "regeneration" after the addition of exogenous 11-cis-retinal.

Regeneration Medium

Crystalline 11-cis-retinal (courtesy of Dr. V. Balogh-Nair, Columbia University) was dissolved in hexane under dim red light: 25 mg into 750 μl. A 30-μl aliquot of this was further diluted with 750 μl of pure hexane; both stock solutions were stored under N_2

TABLE I

*Composition of Bathing Solutions**

	NaCl	KCl	K_2SO_4	$MgSO_4$	$CaCl_2$	$NaHCO_3$	NaH_2PO_4	HEPES	pH	d-Glucose	Other
B_0	135	6	—	2	2	—	—	30	7.4	10	—
B_1	130	5.4	—	1	2	30	1	—	7.8	6	a
B_2	120	3	—	2	2	30	1	—	7.5	5	b
B_3	—	—	3	2	3	—	—	10	7.35	10	c
B_4	120	—	2.7	2	3	—	—	30	—	10	d

* All concentrations are in millimolar.

(a) 0.1 L-ascorbate, 0.1 d-α-tocopherol acetate (dissolved first in ethanol), 0.1 EGTA.

(b) 25 taurine.

(c) 150 Na-isethionate.

(d) 30 sucrose.

atmosphere, light-tight, at −80°C. At the time of each experiment, 75 μl hexane-retinal was pipetted out of the second stock solution into an empty vial, and the hexane was evaporated at room temperature in the dark, by a jet of high-purity, dry nitrogen gas. The 11-cis-retinal was redissolved in 75 μl of absolute ethyl alcohol; this was injected into ~4 ml of N_2-purged saline solution (as described above), which contained pieces of tissue from a 1–3-mm^2 area of retina (cf. Hárosi, 1984).

Spectrophotometer

The dichroic microspectrophotometer (DMSP) has been described (Hárosi and Mac-Nichol, 1974b; Hárosi, 1982a, b). It is a single-beam photometer that simultaneously records average and polarized transmitted fluxes as a function of wavelength between 325 and 695 nm in 5-nm increments. The average transmittance, T, is computed as the ratio of average light fluxes transmitted through sample and reference. Absolute absorbance, A, assumed to be equal to optical density, is computed as $\log(T^{-1})$. Note that this quantity is actually the absorbance of spectral light of the sample relative to that of the reference taken through the suspending medium at a cell-free area in the preparation. Linear dichroism (LD) is obtained as the ratio of alternating to average signal values at each wavelength (cf. Jasperson and Schnatterly, 1969; Treu et al., 1973). With appropriate

amplitude control of the photoelastic modulator (Goode and Buchanan, 1980), LD is proportional to the sample polarization, defined as $p = (T_\| - T_\perp)/(T_\| + T_\perp)$. The LD scale is calibrated with a Rochon prism placed in the light path to produce essentially 100% modulation. Thus, LD = +1.0 for $T_\| = 1$ and $T_\perp = 0$, and LD = −1.0 for $T_\perp = 1$ and $T_\|$ = 0. The dichroic ratio, i.e., the ratio of polarized absorbances ($R = A_\perp/A_\| = \epsilon_\perp/\epsilon_\|$), is determined from A and LD. In a manner analogous to the derivation of Land and West (1946), a formula can be obtained that gives the desired relationship:

$$R = (2\bar{A} + \log k)/(2A - \log k),$$

where

$$k = T_\|/T_\perp = (1 + p)/(1 - p).$$

Although R can be computed for each wavelength segment at which A and LD are known, it is customarily calculated at λ_{max} and is referred to as the cellular dichroic ratio.

Spectral Measurements

The transverse image of the measuring light was a rectangle of ~1 × 3 μm in the specimen plane. The preparation, consisting of a glass sandwich, was placed on the sliding-gliding stage of the DMSP, and in it transversely oriented photoreceptors were searched for under dim red background illumination. A rod or a cone cell would be aligned for measurement longitudinally with the long dimension of the rectangular image, whenever possible, to make the main LD peak positive and the outer segment centered on the beam. The sample transmittance was usually recorded in eight scans (the direction of scanning was mostly violet to red, but it could also be initiated from red to violet or in a sequentially alternating mode). Reference transmittance was recorded in 8 or 16 scans through an adjacent cell-free area. Bleaching (i.e., intentional exposure to actinic light) was performed by an auxiliary beam of a photographers' flashgun (one to three flashes), filtered appropriately, or by the measuring beam, with the monochromator set manually to the desired wavelength (2-min exposure).

Selection Criteria for Spectra

The acceptance or rejection of a record is a critical step in data analysis, and yet distinguishing a "good" spectrum from a "bad" one is not a trivial task (cf. MacNichol et al., 1973, 1983; Hárosi, 1975a; Levine and MacNichol, 1985). If every measured spectrum were merely a statistical variant of the "true" spectrum, there would be no need for selection rules, and each record would have equal weight. However, there are numerous possibilities for "systematic" errors that cause distortions in band shape. Even after all prudent measures have been taken to prevent problems, such as mechanical creep in the microscope focusing adjustment, or in its stage, recorded absorbance spectra often exhibit misshapen bands or large displacements in the baseline. Another problem is progressively increasing apparent absorbance toward shorter wavelengths. This is routinely encountered with small-diameter cells, and is presumably caused by inappropriate focusing, scattering by pigment granules and other cellular debris, and by motion. The last can be of three types: (a) motion in the cell of interest owing to medium streaming caused by thermal gradients, or cell vibrations caused by Brownian bombardments; (b) preparation volume changes caused by shrinkage or expansion in trapped air bubbles, or by a leaky seal in the enclosure; (c) wavelength-dependent movements of the measuring beam caused by the imperfect alignment of grating or mirrors, and incomplete correction for chromatic aberrations in the condenser and objective. Gross spectral distortions can often be visually traced to cell motion, but the cause of subtler distortion may go undetected.

The acceptance of a visual pigment spectrum has been traditionally decided by two criteria: (a) shape conformity; i.e., the width of the α-band in question should be similar to that of others; and (b) baseline conformity; i.e., the absolute absorbance on the longwave limb of the α-band should approach a value not exceeding ~10% of the peak. The same two criteria were applied in this study not only to the absolute absorbance spectra, but also to the bleaching difference and linear dichroism spectra, whenever possible. The actual screening of records involved no manipulation by hand. If the shape and baseline criteria were satisfied by visual scrutiny, the spectrum was processed by the program FILTER (see below). This program quickly established the relevant parameters. A new feature in FILTER is that it resolves the bandwidth of the α-band peak into two segments: the longwave half-density (LWHDBW), plus the shortwave half-density (SWHDBW), equaling the total half-density bandwidth (THDBW). The THDBW, or simply "band-width" (also called the "half-bandwidth"), is the abscissa difference (in wavenumbers) between two vertices at which the ordinates are 50% of the peak. The reason for splitting the bandwidth into two parts is twofold. First, it permits direct comparisons between published results (e.g., Bowmaker et al., 1980) on the LWHDBW and those obtained here. Second, it facilitates the screening of records, including those in which the SWHDBW did not exist owing to high photoproduct absorbance or excessive scattering. It was observed in this study that the LWHDBW usually has the smallest variance; consequently, the longwave side of the α-band is the least variable and thus the most reliable portion of the spectrum. The standard deviation of the LWHDBW was used as a measure of acceptability for the spectra.

Fourier Filtering

Digital filtering by using Fourier transformation of wavelength spectra was developed following the method described by Bush (1974). Since light absorption of visual pigments is always a slowly varying function of wavelength, the apparent rapid fluctuations in their spectral absorbance can be attributed to noise. It is further assumed that this noise is random, having an essentially "white" power spectrum. Consequently, when a noisy wavelength spectrum is Fourier-transformed into an equivalent frequency domain, the major harmonic components of the "signal" and those of the "noise" can be segregated on a frequency basis. For the simulation of a rectangular low-pass filter characteristic, the operator can select the number of long-period Fourier coefficients to be retained. Automatic selection of the cutoff point was also implemented (cf. Bush, 1974) by computing the standard deviation in amplitude for subsets of higher-order terms in a sequential manner. First, the upper 32 (highest frequency) elements of the complex data array were used in the computation; then successively lower-order terms were added in and the standard deviation was recalculated each time. As long as the included coefficients represent mainly noise, the standard deviation is independent of their number. If, however, coefficients with signal content are also included, the computed standard deviation will rise above the value found for noise alone. The process is continued until the ratio of two standard deviations obtained in sequence (SD_{new}/SD_{old}) exceeds a certain criterion value (1.03–1.20). All higher-frequency coefficients above the last term plus two are set to zero, the inverse Fourier transform is calculated from the remaining terms, and the linear trend is restored (see below).

The program named FILTER was written in FORTRAN code, edited, and compiled under the RT-11 operating system of a PDP-11/23 computer (Digital Equipment Corp., Maynard, MA). The first requirement, that the data be equally spaced in wavelength, was fulfilled by the original design of the DMSP. FILTER was planned to accommodate sets of up to 128 spectral points. The experimental data are filed into arrays of 75 pairs of numbers (obtained in single or multiple scans) signifying A, LD, or BD absorbance values

and their corresponding wavelengths. At the discretion of the operator, the data can first be subjected to a recursive, weighted (three-point) average filter. Next, the data are "detrended"; this is done by averaging the last three points at both ends of the range, computing a linear trend between them, and subtracting an appropriate value from every ordinate at each abscissa (cf. Bush, 1974). The data array is then padded on the long-wavelength side with the last detrended value to expand the array to 128 points, and transformed into a reciprocal wavelength domain by the fast Fourier transform (e.g., Robinson, 1967). The resulting complex array is used for the calculation of standard deviations of the Fourier coefficient amplitudes. The number of complex coefficient pairs to be retained can be obtained automatically if a criterion ratio is specified, as outlined above, or can be set by the operator. In either case, the higher-frequency terms are set equal to zero, and the inverse Fourier transform (via the same subroutine) is performed on the array. The resulting spectrum is a smoothed representation of the initial data set.

In order to find the wavelength corresponding to the maximum, a third-degree polynomial (Bevington, 1969) is fitted to seven points (±15 nm) around the smoothed peak, followed by interpolation of the largest ordinate to the nearest 0.05 nm. The abscissa corresponding to the half-maximum ordinate on each limb of the peak is searched for in an array obtained by the linear interpolation of the three points nearest the nominal 50% ordinate value, again to a resolution of 0.05 nm.

Experience with this FILTER program showed that the A, BD, and LD spectra of visual pigments can be smoothed rapidly (in a few seconds). At a prescribed standard deviation ratio of 1.10, it usually returns the lowest 8 (±3) pairs of complex Fourier coefficients out of the total of 64. The inverse transform of these pairs results in a smooth rendition of the experimental spectrum, which compares favorably with those obtained via the more elaborate method of curve-fitting to linear combinations of three or four Gaussian functions (Hárosi, 1976). That method requires the preselection of three parameter values for each Gaussian component, and the fitted result is somewhat dependent on the initial choices. Smoothing by FILTER is free of such arbitrariness. Nevertheless, a degree of variability may be present here also. This occurs (a) if the operator sets unreasonably high criterion values to be used in the automatic cutoff determination, (b) if he forces the number of terms (t) to be an exaggerated one, or (c) when the data points at either end of the spectral range are excessively noisy. Erratic end points cause erratic detrending, which in turn yields an erroneous Fourier representation. The solution of choice was to discard wildly fluctuating data values from either or both ends of the spectrum. The shortwave end, which is naturally noisy because of the meager number of photons available in the light source, generally required the disallowance, on average, of five or six points. Noisy values on the longwave end (probably caused by transients of external origin) were infrequent, and rarely needed more than one or two points to be deleted. Prefiltering, by the use of the recursive weighted averaging routine, was found to be unnecessary except for the noisiest of spectra.

Statistical Analyses

Individual processing of a spectrum resulted in the determination of four parameters: λ_{max}, LWHDBW, SWHDBW, and THDBW. For each cell type and class of spectrum, these parameters were averaged; the sample mean, variance, and standard deviation were routinely calculated. The sample distribution of λ_{max} for the green and red cone absorbance spectra of cynomolgus were investigated by an analysis-of-variance test for normality developed by Shapiro and Wilk (1965). The Shapiro and Wilk test, which is an assessment against a null hypothesis that the values in question are from a normal population, was used.

The population mean λ_{max} for each type of pigment was determined according to the

following scheme. (a) The compiled data were reviewed and the most significant sets were selected. The determinations chosen were those that had the largest number of samples, those that had finite parameter values, and those that were most likely to be independent of one another. (b) The variance ratio test was performed to ascertain whether the sample variances were sufficiently alike to warrant the assumption that they were independent estimates of the same population variance. (c) The population variance was estimated by pooling the sample information (under the assumption that the samples were drawn from a common parent population). (d) The difference between the sample means was investigated by calculation of the Student's t test. This was done by dividing the difference of means by the standard error of the difference (based on the best estimate of the standard error for the difference of means). (e) When the means were found to be significantly alike by the latter test, the samples were pooled to arrive at a global mean. The standard error was then calculated from the pooled variance (established under c), based on the total degrees of freedom and the t scores for the 95% level of certainty.

RESULTS

Cynomolgus Rods

A total of 62 permanent records were obtained from cynomolgus rods. Of these, 56 were identified as single cells; the remaining 6 recordings were derived from doubly or multiply overlapping structures. Among the single rods, 12 were recognized as "super rods" (Hárosi, 1982a; MacNichol et al., 1983). Whereas a common rod, when well preserved, is seen to have an outer segment of ~1–1.5 μm diam, a super rod may have twice that dimension (see Fig. 1). Also, super rods have larger A and LD values, as well as a higher dichroic ratio.

Common rods. The 50 common-rod records consisted of 44 single-cell, 2 double-cell, and 4 multiple-cell or edge-fold measurements. Most of the absolute absorbance spectra from among the single-cell records turned out to be distorted—typically by an elevated baseline—even at long wavelengths, where rhodopsin is known to have negligible absorbance. The three best absolute absorbance spectra (each of which consisted of summed signal values for eight scans) from single rods were averaged and smoothed by FILTER. The results are shown as trace a in Fig. 2A and in entry 1 of Table II. The corresponding three LD spectra were also averaged and smoothed (not shown). The dichroic ratio was then calculated from the peak A and LD and found to be 3.28, a respectably high value, similar to those seen in the rods of fish (e.g., Hárosi and Hashimoto, 1983). Trace b in Fig. 2A is the average of two absorbance spectra derived from multiple rods. The spectral data determined from the smoothed curve are given in entry 2 of Table II. The corresponding average of the two LD spectra permitted the calculation of the dichroic ratio for the edge-fold case; it was 2.28. In contrast to the paucity of distortion-free absorbance spectra, LD measurements had better yields. The spectrum depicted in Fig. 2B was obtained as the average of 11 eight-scan records, 9 of which were from single rods and 2 from doubly overlapping ones (cf. entry 3 of Table II). The same 11 LD spectra were also processed by FILTER one by one and then their parameters were averaged; the results are shown in entry 4 of Table II. A successful BD spectrum determined from a globular stump of an outer segment yielded a positive maximum at 501.5 and a negative peak at 384 nm (cf. entry 5 of Table II).

Super rods. These cells were found in six animals, males and females, ranging in age from 2 to 5 yr. In one experiment, the retinal sample in which a super rod appeared was definitely identified as peripheral; in other instances, the original location of the tissue within the retina could not be reconstructed. While all must have come from extrafoveal regions, their retinal distribution remained undetermined. 6 out of the 12 cells provided seven useful eight-scan absolute absorbance spectra. Their average furnished the data in entry 6 of
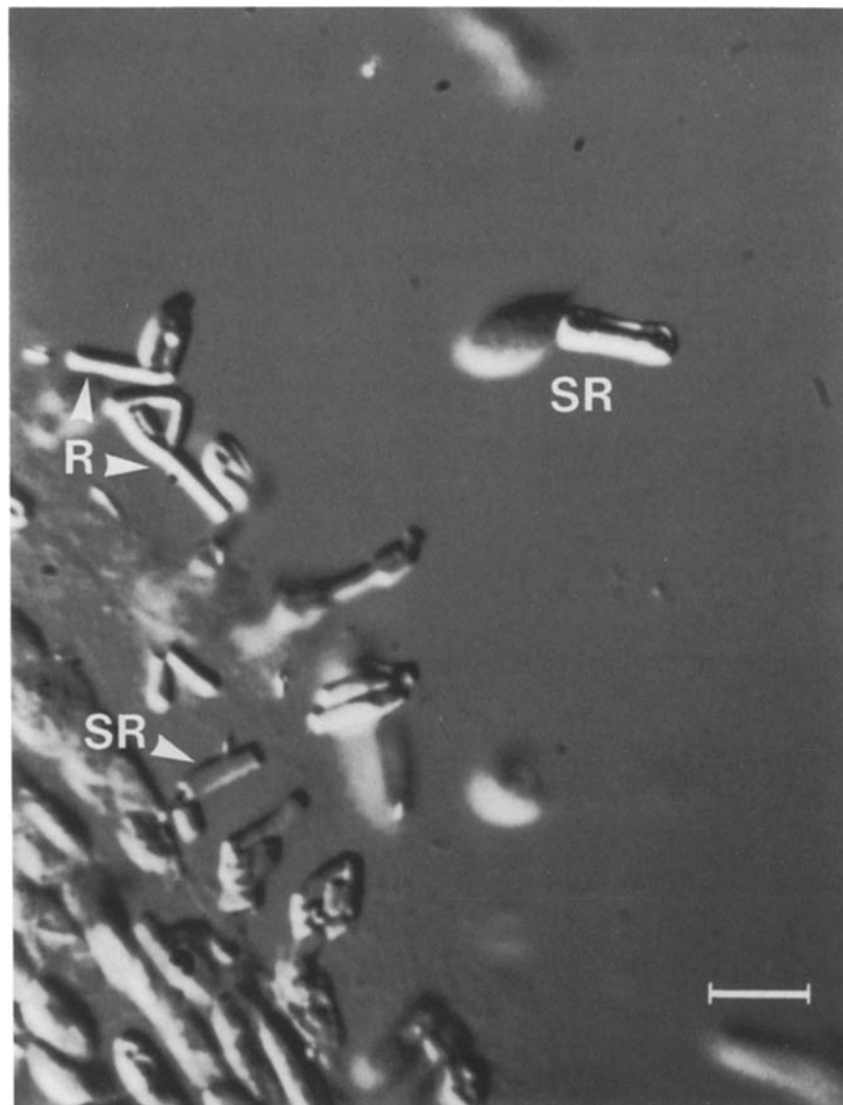
FIGURE 1.   Cynomolgus retinal rods photographed in a Nomarski differential interference-contrast microscope (Carl Zeiss, Inc., New York). R, common rod. SR, super rod. Calibration bar, 10 μm. (Photo courtesy of B. A. Collins.)

Table II. The average of the best four of these records is depicted in Fig. 3 A. The spectral data corresponding to this average (entry 7) and the result of individual processing (entry 8) are also included in Table II. The average LD spectrum obtained from four super-rod outer segments is shown in Fig. 3 B; their
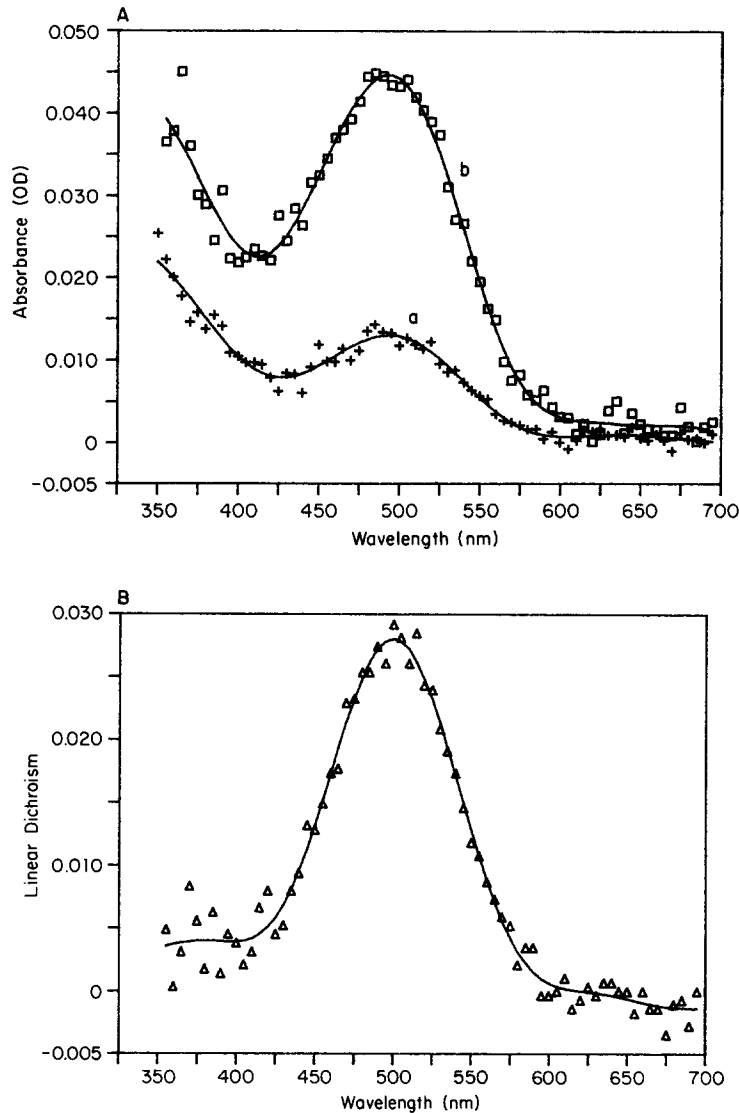
FIGURE 2.   Common rod spectra in cynomolgus. (A) Absolute absorbance. Trace a: average of three eight-scan single-cell recordings (crosses). The solid curve is produced by Fourier smoothing. Criterion (cr) = 1.1; retained number of lower frequency terms (t) = 8. Trace b: average of two eight-scan edge-fold spectra (squares). The solid curve is the result of Fourier smoothing (cr = 1.1, t = 8). (B) Linear dichroism; average of 11 eight-scan recordings (cr = 1.1, t = 8).

parameters are listed in entry 9 of Table II. After the averaging of the corresponding four absorbance spectra, the dichroic ratio was calculated at the peak A and LD and found to be 2.68. The same calculation, however, yielded 3.77 for the best super-rod measurement. The latter value is remarkably high and rivals those of the most dichroic amphibian photoreceptors (e.g., Hárosi, 1976).

4 out of the 12 super rods were located under "regenerating" conditions. BD spectra were obtained from two of them; one of these is depicted in Fig. 3 C. This spectrum has a maximum at 504.8 nm and a minimum at 373.5 nm. The width of the positive peak (α-band) is broader than expected (cf. entry 10 of Table II) and has a "shoulder" near 450 nm, where a metarhodopsin III–like photoproduct might be involved.

TABLE II
Cynomolgus Rod Spectral Data

Entry	Spectrum type	Description	λ_{max}	SWHDBW	LWHDBW	THDBW
			nm	cm^{-1}	cm^{-1}	cm^{-1}
	Common rods					
(1)	A	($n = 3$)	493.8	—	1,839	—
(2)	A	($n = 2$; edge-fold)	493	3,354	1,888	5,242
(3)	LD	($n = 11$)	500.3	2,129	1,718	3,847
(4)	LD	Processed singly*	500.7±4.3	2,241±267	1,751±83	3,992±294
(5)	BD	($n = 1$)	501.5	2,282	1,639	3,921
	Super rods					
(6)	A	($n = 7$; 6 cells)	496.8	—	1,767	—
(7)	A	($n = 4$; 3 cells)	498.3	3,335	1,706	5,041
(8)	A	Processed singly*	496.7±3.8	2,630±218 (3)	1,730±70	4,374±290 (3)
(9)	LD	($n = 4$)	501.3	2,130	1,704	3,834
(10)	BD	($n = 1$)	504.8	2,376	1,940	4,316

* Sample mean ± 1 SD (the number of samples, if different from the description, is in parentheses).

Cynomolgus Blue-absorbing Cones

A total of 12 cynomolgus cone outer segment stumps revealed peak absorbance in the blue part of the spectrum. Several of them permitted multiple measurements; eight yielded useful records, while all spectra obtained from the remaining four cells were rejected. Even though the spectrum acceptance criteria were relaxed for baseline offsets, the unacceptable ones were deemed so because of the presence of precipitously rising apparent absorbance toward shorter wavelengths. These cells were found in various bathing media; three of them were located in suspensions to which exogenous 11-*cis*-retinal was added. BD spectra were obtained from six cells.

Absolute absorbance spectrum. The average of 11 eight-scan recordings obtained from six cells is shown in Fig. 4A (cf. entry 1 of Table III). Entry 2 of Table III shows the results of individual processing. The outcome of a more stringent selection (see Methods), in the course of which only seven records from
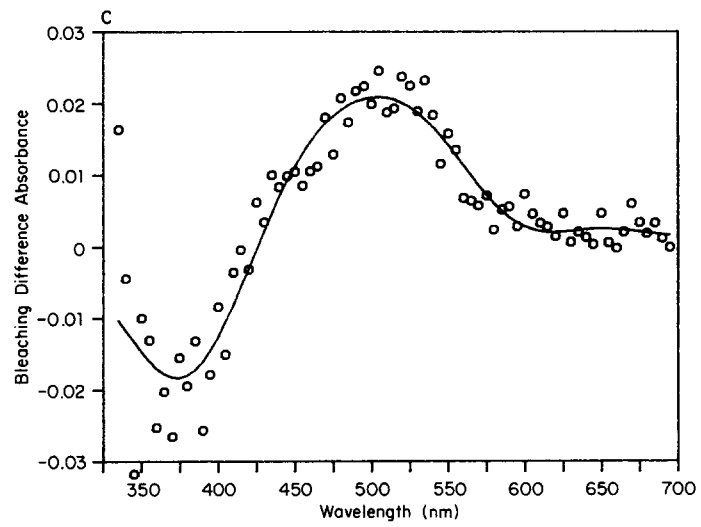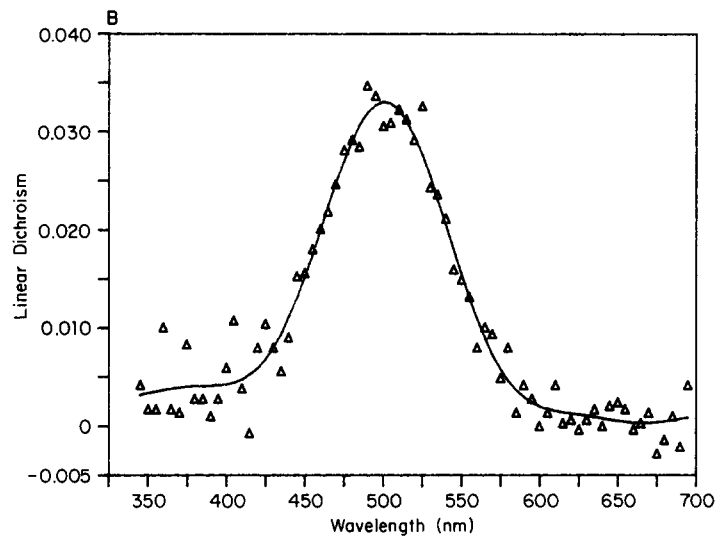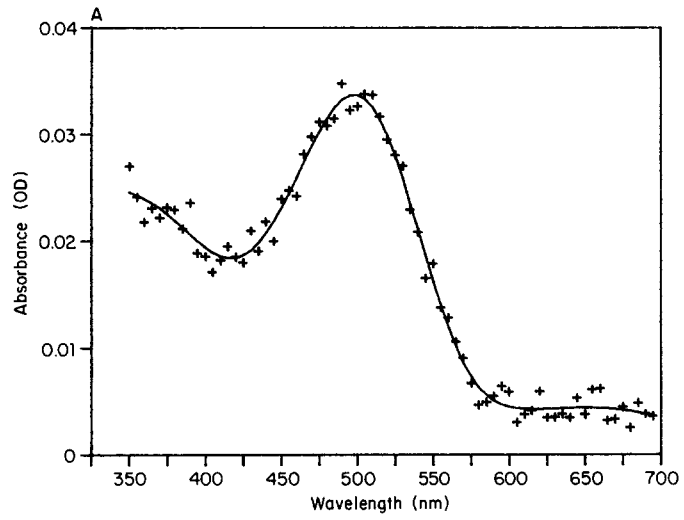
four cells were retained, is given in entries 3 and 4 of Table III. The "best" average of four eight-scan spectra derived from four separate stumps was also analyzed (not shown). Data computed from the smoothed curve and from the individually processed ones are listed in entries 5 and 6 of Table III.
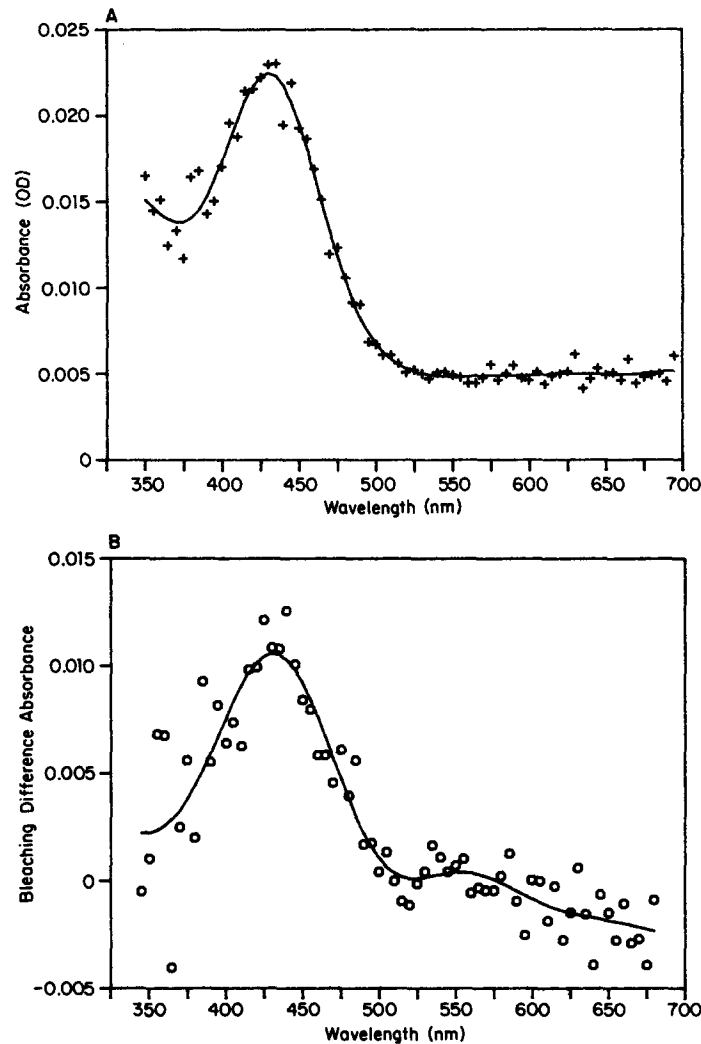
FIGURE 4. Blue-absorbing cone spectra in cynomolgus. (A) Absorbance spectrum; average of 11 eight-scan recordings obtained from six cells (cr = 1.1, t = 10). (B) Bleaching difference; average of four determinations (cr = 1.1, t = 7).

FIGURE 3. (*opposite*) Super-rod spectra in cynomolgus. (A) Absolute absorbance; average of four eight-scan measurements from three single cells (cr = 1.1, t = 9). (B) Linear dichroism; average of four eight-scan determinations obtained from four single cells (cr = 1.1, t = 8). (C) Bleaching difference; the prebleach and postbleach recordings were averaged from eight spectral scans (cr = 1.1, t = 6).

Bleaching difference spectrum. Out of the six blue cone stubs bleached in the DMSP, five yielded useful BD spectra, two being doubly recorded. The average of these seven BD records resulted in the data shown in entry 7 of Table III. When they were Fourier-filtered one by one, the data were as indicated in entry 8 of Table III. Using more stringent criteria for acceptance, a total of four BD spectra were selected; their average and the Fourier-filtered curve are depicted in Fig. 4*B*. The data determined from their average and individual processing are given in entries 9 and 10 of Table III.

Linear dichroism. As mentioned in the Introduction, cone outer segments appeared to lose their structural integrity and, concomitantly, most of their linear dichroism within the first hour of enucleation in these experiments. Four blue cone remains exhibited faint linear dichroism: one had a positive and three

TABLE III

Cynomolgus Blue-absorbing Cone Spectral Data

Entry	Spec- trum type	Description	λ_{max}	SWHDBW	LWHDBW	THDBW
			nm	*cm^{-1}*	*cm^{-1}*	*cm^{-1}*
(1)	A	(*n* = 11; 6 cells)	430.5	—	1,920	—
(2)	A	Processed singly*	430.4±6.1	2,308±301 (7)	2,002±357	4,089±371 (7)
(3)	A	(*n* = 7; 4 cells)	431	2,393	1,802	4,195
(4)	A	Processed singly*	431.7±5.3	2,285±323 (6)	1,864±310	4,047±388 (6)
(5)	A	(*n* = 4)	430.8	2,204	1,795	3,999
(6)	A	Processed singly*	429.2±5.7	2,057±256 (3)	1,981±387	3,873±505 (3)
(7)	BD	(*n* = 7; 5 cells)	432.8	2,484	1,831	4,315
(8)	BD	Processed singly*	430.3±10.2	2,526±532 (6)	2,091±460	4,477±799 (6)
(9)	BD	(*n* = 4)	431.3	2,718	2,018	4,736
(10)	BD	Processed singly*	429.9±3.0	2,657±754 (3)	2,237±528	4,663±1,066 (3)
(11)	LD	(*n* = 3)	426.5	2,096	1,745	3,841

* Sample mean ± 1 SD (the number of samples, if different from the description, is in parentheses).

others a negative peak for the expected α-band. Whereas the sign of an LD band is a mere indication of the relative geometry of the measurement with respect to the axes of symmetry in the sample, the presence of LD in a dark-adapted cell, be it positive or negative, means anisotropic absorption; this, combined with the optical purity of vertebrate rod and cone outer segments, is taken as evidence of a visual pigment. Three of the obtained LD spectra with the same sign were averaged; the computed parameters are listed in entry 11 of Table III. The dichroic ratio was also calculated for the average of the two "best" LD and corresponding A spectra and found to be 1.33. Although this value is much lower than those of monkey rods or fish cones, it is comparable to the dichroic ratios obtainable from the other cone types (see below).

Cynomolgus Green-absorbing Cones

The outer segment stumps of 47 cones had absorbance peaks in the midwave region. 21 of these cells furnished 34 useful spectra.

Absolute absorbance spectrum. 18 absolute absorbance spectra were scrutinized one by one, 3 of which were eventually rejected for subtle distortions indicative of movement artifact. The 15 remaining spectra, obtained from 13 cells, were each processed by FILTER and their parameters were averaged. The mean values of the LWHDBW and the SWHDBW thus established were then used as references, and the individual records were screened again for aberrant widths. Spectra whose half-bandwidths were outside the mean ± (1–1.5) SD became suspect and were set aside. The remaining seven single-cell records were averaged and smoothed, as well as individually processed; the results are shown in entries 1 and 2 of Table IV. In view of the possibility that anomalous green and red pigments may be present in macaques (Bowmaker et al., 1978, 1980; MacNichol et al., 1983), deviant spectra were not discarded automatically. To

TABLE IV

Cynomolgus Green-absorbing Cone Spectral Data

Entry	Spectrum type	Description	λ_{max}	SWHDBW	LWHDBW	THDBW
			nm	*cm^{-1}*	*cm^{-1}*	*cm^{-1}*
(1)	A	(n = 7)	533.3	2,549	1,604	4,153
(2)	A	Processed singly*	533.1±3.6	2,559±162	1,627±124	4,186±272
(3)	A	(n = 15; 13 cells)	532.8	2,407	1,615	4,022
(4)	A	Processed singly*	532.7±3.2	2,484±254 (13)	1,661±129	4,157±309 (13)
(5)	BD	(n = 4)	535	2,148	1,554	3,702
(6)	BD	Processed singly*	534±2.2	2,241±333	1,572±81	3,813±403
(7)	LD	(n = 3)	521.3	2,460	1,805	4,265

* Sample mean ± 1 SD (the number of samples, if different from the description, is in parentheses).

see the effect of the remaining records upon the previous selection, all 15 of them were treated as samples from one population; their average is depicted in Fig. 5A. The spectral parameters of the average curve and of the individually processed ones are listed in entries 3 and 4 of Table IV. A comparison of the data in the first four entries of this table reveals that, although the parameter standard deviations changed somewhat when the sample size was increased from 7 to 15, the mean values remained virtually unchanged. This implies a lack of bias in the selection process. The application of the Shapiro and Wilk (1965) test to the distribution of λ_{max} values showed no evidence for non-normality that might indicate a second population of green cones ($W = 0.949$).

Bleaching difference spectrum. Successful experiments of this type were carried out on seven green-absorbing cynomolgus cones. Before bleaching, each of these cells was measured at least once in eight spectral scans, three of them being recorded twice. The postbleach measurement of each was used as the reference in computing the absorbance of its respective first prebleach spectrum. The best four BD spectra were averaged and smoothed to yield Fig. 5B and the data in entry 5 of Table IV; their individual processing resulted in the data of entry 6.

Linear dichroism. A total of six eight-scan recordings had a perceptible

A

Absorbance (OD)

0.035
0.030
0.025
0.020
0.015
0.010
0.005
0

350 400 450 500 550 600 650 700
Wavelength (nm)

B

Bleaching Difference Absorbance

0.03
0.02
0.01
0
-0.01

350 400 450 500 550 600 650 700
Wavelength (nm)

C

Linear Dichroism

0.015
0.010
0.005
0
-0.005
-0.010

350 400 450 500 550 600 650 700
Wavelength (nm)
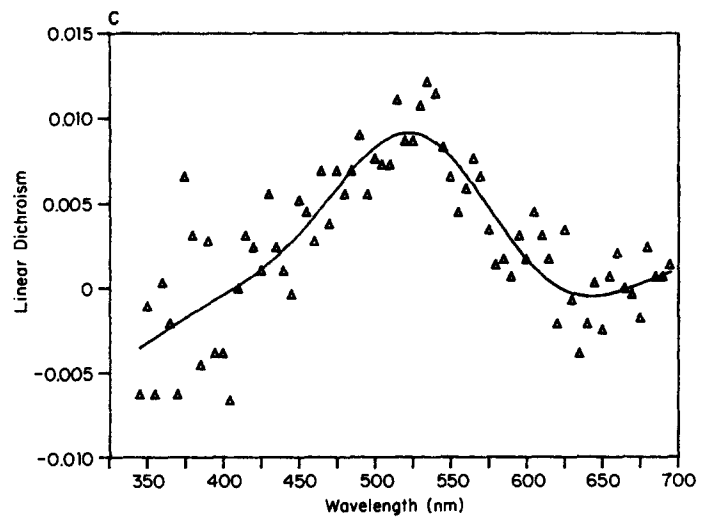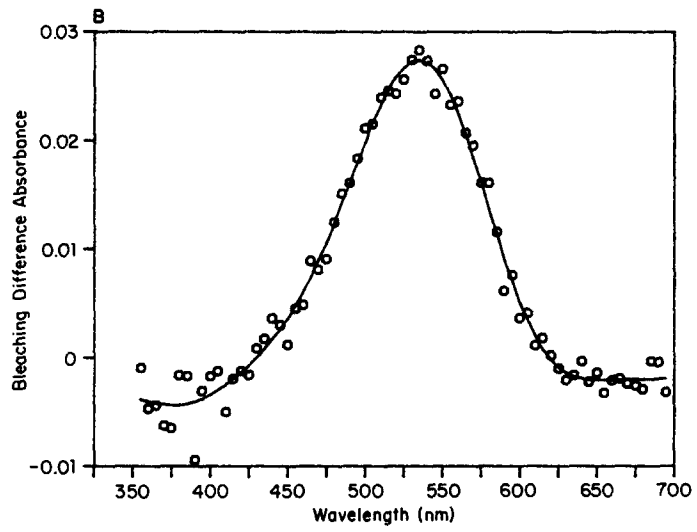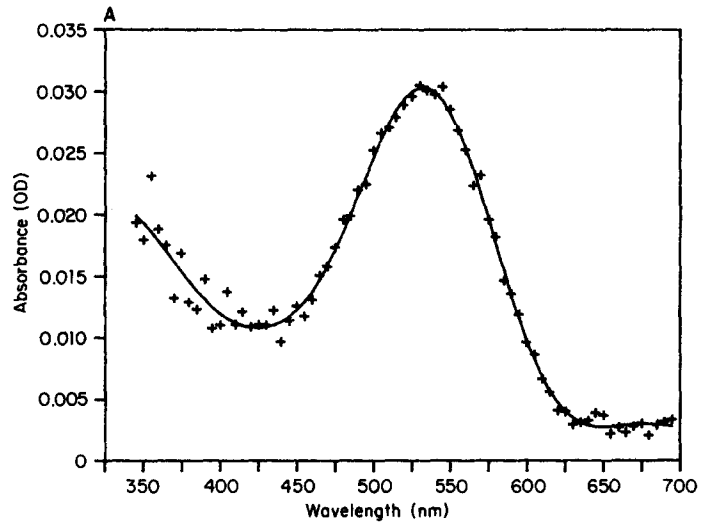
anisotropic response in the α-band. Three of the better ones were averaged and smoothed by FILTER; the results are shown in Fig. 5C and entry 7 of Table IV. The corresponding three absorbance spectra were also averaged so that the mean dichroic ratio could be calculated. It was 1.43, a value similar to the dichroic ratio found above for the blue cones.

Cynomolgus Red-absorbing Cones

44 cynomolgus cone outer segment stumps were measured with α-band peaks in the longwave region. 30 of these structures yielded 57 spectra that appeared to be worthy of further scrutiny.

Absolute absorbance spectrum. 16 of the 24 records of this type, obtained from 20 cells, were Fourier-filtered one by one. 11 of them were deemed acceptable; their average spectrum is depicted in Fig. 6A. The λ_{max} of the smoothed curve was determined at 566 nm (entry 1 of Table V). When the same 11 spectra were filtered first and the parameters were averaged, the mean λ_{max} was found at a slightly lower value of 564.9 ± 5.6 nm, as shown in entry 2 of Table V. The Shapiro and Wilk (1965) normality test applied to the λ_{max} data resulted in the W statistic having a value of 0.971. This is just below the 90% point of the null distribution (0.973, $n = 11$), and thus, here again, there is no evidence of non-normality. To probe further into the nature of the variation among the spectra, the parameters of the 16 individually smoothed curves were averaged in two additional combinations. The results are listed in entries 3 and 4 of Table V. These data suggest that the inclusion of more deviant spectra had minor effects on the mean λ_{max}, but tended to cause standard deviation increases in the bandwidths. The conclusion, therefore, is that the deviant curves straddle the mean with about equal probability of being on either side of the peak. The data thus provide no evidence for the existence of a bimodal distribution of λ_{max} in cynomolgus red cones.

Bleaching difference spectrum. 16 of the 44 red-absorbing structures were bleached. From among the 24 postbleach records, only 13 survived the initial screening. Further scrutiny reduced the number of acceptable BD spectra to five; their average is shown in Fig. 6B and the computed parameters are listed in entry 5 of Table V. Individual processing of the same five spectra yielded the data in entry 6 of Table V.

Linear dichroism. Perceptible anisotropic modulation was found in nine spectral recordings obtained from seven amorphous protuberances of the red-absorbing type. Only three of these were averaged to yield the data in entry 7 of Table V. The corresponding three absorbance spectra were also averaged so that the dichroic ratio could be determined. It was 1.52, a value constituting the largest dichroic ratio obtained for cones in the course of this study.

FIGURE 5. (*opposite*) Green-absorbing cone spectra in cynomolgus. (A) Absolute absorbance; average of 15 eight-scan recordings (cr = 1.1, t = 8). (B) Bleaching difference; average of four determinations (cr = 1.1, t = 8). (C) Linear dichroism; average of three eight-scan recordings from as many structures (cr = 1.1, t = 5).

Rhesus Rods

22 records were saved from among the rhesus rod measurements. 17 of these were obtained from single rod outer segments; the rest were from two or more overlapping rods. None of these cells were either bleached or regenerated. Although the absolute absorbance spectra did not meet the acceptance criteria, some of the LD spectra did. 10 such records were analyzed; the results are listed
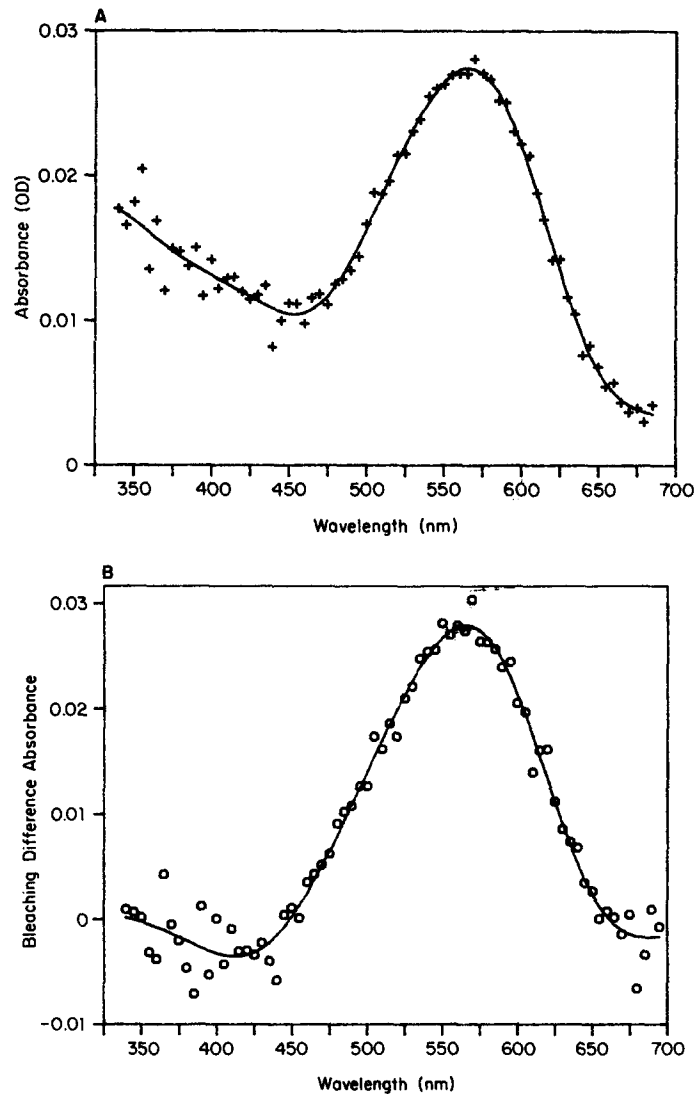
FIGURE 6.   Red-absorbing cone spectra in cynomolgus. (*A*) Absolute absorbance; average of 11 single-cell records (cr = 1.1, *t* = 8). (*B*) Bleaching difference; average of five eight-scan spectra (cr = 1.1, *t* = 7).

TABLE V

Cynomolgus Red-absorbing Cone Spectral Data

Entry	Spectrum type	Description	λ_{max}	SWHDBW	LWHDBW	THDBW
			nm	*cm⁻¹*	*cm⁻¹*	*cm⁻¹*
(1)	A	(n = 11)	566	2,465	1,518	3,983
(2)	A	Processed singly*	564.9±5.6	2,460±410	1,535±124	3,995±403
(3)	A	Processed singly* (n = 12)	565.2±6.1	2,462±409 (11)	1,498±123	3,963±415 (11)
(4)	A	Processed singly* (n = 16)	564.1±6.2	2,524±394 (15)	1,572±179	4,103±453 (15)
(5)	BD	(n = 5; 4 cells)	565.8	2,318	1,508	3,826
(6)	BD	Processed singly*	564.6±3.1	2,374±323	1,566±103	3,940±391
(7)	LD	(n = 3)	570.3	2,428	1,562	3,990

* Sample mean ± 1 SD (the number of samples, if different from the description, is in parentheses).

in entries 1 and 2 of Table VI. The dichroic ratio calculated from the peaks of the LD and the corresponding average absorbance was 2.77.

Rhesus Blue-absorbing Cones

A total of five rhesus cone outer segment remains were found with elevated absorption in the blue spectral region; however, the recordings from one of

TABLE VI

Rhesus Rod and Cone Spectral Data

Entry	Spectrum type	Description	λ_{max}	SWHDBW	LWHDBW	THDBW
			nm	*cm⁻¹*	*cm⁻¹*	*cm⁻¹*
	Rod					
(1)	LD	(n = 10)	500.5	2,119	1,700	3,819
(2)	LD	Processed singly*	500.8±5.9	2,222±293	1,739±80	3,960±350
	Blue-absorbing cone					
(3)	A	(n = 2)	430	—	—	—
(4)	BD	(n = 2)	431	—	—	—
	Green-absorbing cone					
(5)	A	(n = 1)	535	2,439	1,567	4,006
(6)	A	(n = 3)	534.5	—	1,621	—
(7)	A	Processed singly*	534.3±0.8	—	1,634±90	—
(8)	BD	(n = 1)	535.5	2,161	1,576	3,737
	Red-absorbing cone					
(9)	A	(n = 3)	567	2,183	1,458	3,641
(10)	A	Processed singly*	566.8±0.8	2,182±234	1,482±52	3,664±190
(11)	BD	(n = 2)	565	2,409	1,538	3,947
(12)	LD	(n = 3)	569.3	3,032	1,623	4,655

* Sample mean ± 1 SD.

them were lost by inadvertent erasure from memory. One of the remaining four cones was located in a preparation that was supplemented with 11-*cis*-retinal, while three of the four outer segment stumps were bleached. Because of baseline offsets and distortions, the records did not meet the acceptance criteria. They were analyzed nevertheless, with the results shown in entries 3 and 4 of Table VI. Linear anisotropy was detected in only one record of poor quality.

Rhesus Green-absorbing Cones

13 cones were found in rhesus preparations with light absorption in the midwave region of the spectrum. A total of eight recordings were considered for further analysis: three A, two BD, and three LD spectra. The data for the best absorbance spectrum are shown in entry 5 of Table VI. The analysis of the three A spectra yielded the results in entries 6 and 7. The BD spectrum, which was obtained from a cone located in a regeneration medium, provided the data in entry 8. LD responses were found in three cells; their average provided the peak LD for the calculation of, combined with the corresponding average A peak, the dichroic ratio. It was found to be 1.34—a low, but not unusual, value for deteriorating cones.

Rhesus Red-absorbing Cones

Permanent records were obtained from 13 longwave-absorbing cones. Six of these cells were found in media supplemented with ethanolic solutions of 11-*cis*-retinal. Whereas 4 of the 13 cells were bleached to provide BD spectra, only 3 structures yielded detectable LD responses. The three acceptable absorbance spectra were analyzed; the data are shown in entries 9 and 10 of Table VI. Both of the two acceptable BD spectra were obtained from cells that were incubated and mounted in a regeneration medium. Their average yielded the data in entry 11. Entry 12 shows data obtained from the three LD spectra. The dichroic ratio was determined to be 1.25. This again is a low value, albeit not exceptionally so.

DISCUSSION

Peak Absorbance of the α-Bands

The smoothing of spectra by Fourier transformation appears to be an excellent method for the removal of rapid fluctuations, although it is less effective against low-frequency noise. For obvious reasons, noise and signal with overlapping power spectra cannot be completely separated on the basis of frequency. Nevertheless, signal enhancement relative to random events is still possible by increasing the number of observations and averaging them. Although both the Fourier transformation and averaging are linear operations, they may lead to slightly different results, depending on the sequence in which the operations are performed. Because averaging reduces random fluctuations at all frequencies, it is advantageous to average as large a number of records as possible first and then smooth by FILTER. The parameters obtained this way are believed to be the more accurate. Data arrived at by averaging individually processed spectra, on the other hand, are useful in the estimation of scatter.

Cynomolgus Rod Pigment λ_{max}. The spectral parameters compiled in Table II show no systematic difference between the rhodopsins contained in rods, regardless of their size. The most reliable data on rods were invariably obtained from LD recordings. Because the common rod *A* spectra tended to have artificially high shortwave values and the BD spectra were scarce, only the parameter values listed in entries 3, 4, 7, and 8 of Table II were used. After the procedure outlined in the Methods, the mean λ_{max} and the standard error of the mean at the 95% confidence interval were found to be 499.7 ± 2.5 nm.

Cynomolgus Blue Cone Pigment λ_{max}. *A* and BD spectra were always the most reliable ones obtainable from cones. The parameters in entries 1, 2, 7, and 8 of Table III were used in the analysis, giving a λ_{max} value of 431.4 ± 4.2 nm.

Cynomolgus Green Cone Pigment λ_{max}. The *A* and BD spectral data were taken from entries 1, 2, 5, and 6 of Table IV. Once again, no statistical difference was found between the two sets of data. The mean λ_{max} was 533.9 ± 2.4 nm.

Cynomolgus Red Cone Pigment λ_{max}. Data from the entries 1, 2, 5, and 6 of Table V were used in this analysis and, just as before, no statistically significant difference was found between the *A* and BD averages. The pooled λ_{max} and its standard error were 565.9 ± 2.8 nm.

Rhesus Rod and Cone Pigment λ_{max}. Since only ~30% as many photoreceptors were measured in the rhesus as in the cynomolgus, the obtained parameter values carry less weight. Nonetheless, the spectra of rhesus rods and cones in each class were always commensurate with the means and error margins established for the cynomolgus pigments (see Table VI). Because no statistically significant difference was found between the optical spectra of the two species, their visual pigments can be regarded as spectrally identical.

In a preliminary report of this work (Hárosi, 1982a), the λ_{max} values of the rods and blue, green, and red cone pigments in both species were estimated at 498 ± 2, 430 ± 5, 532 ± 2, and 563 ± 2 nm, respectively. These figures were based on the analysis of a few spectra selected from among the initial 40% of the records now on hand. Since neither extensive averaging nor statistical methods were used and, moreover, the Fourier smoothing program was unavailable at the time, the currently determined results are the more reliable.

Because thorough appraisals of the earlier efforts on primate visual pigments have been published (e.g., MacNichol et al., 1973, 1983; Bowmaker et al., 1978), the following discussion is limited to the most recent and relevant studies. Bowmaker et al. (1978) found no blue-absorbing cones in rhesus; their λ_{max} values for rods and green and red cones were 502 ± 2.5, 536 ± 3.5, and 565 ± 2.5 nm. Bowmaker et al. (1980) reported on cynomolgus visual pigments: on the basis of two blue cone recordings, they determined the peak at 415 nm, while they arrived at 500.1 ± 1.6, 533.3 ± 3.9, and 567 ± 6.1 nm for the rods and green and red cones, respectively. In contrast to the above, MacNichol et al. (1983) found the blue pigment of the cynomolgus with λ_{max} near 430 nm. From a total of eight blue cones, three were judged suitable for analysis; their average λ_{max} was 429 ± 4 nm. In a subsequent report based on a larger data pool, Mansfield et al. (1984) obtained 426 ± 3.4 nm for the average *A* peak of shortwave cones (seven cynomolgus and three rhesus). The λ_{max} for the average

BD spectrum from four cynomolgus and two rhesus blue cones was 434 ± 6.6 nm. Although in the present study, smaller differences than these were found between A and BD spectra (cf. Table III), their λ_{max} values and those of the present work are in good agreement.

Anomalous green cone pigments were reported by Bowmaker et al. (1978) in rhesus and by MacNichol et al. (1983) in cynomolgus (from retinas fixed in glutaraldehyde). In the course of this study, only unfixed and relatively fresh tissue was measured, and the λ_{max} values of the green and red cone data revealed no evidence of any subpopulation in their spectra. These results, therefore, are only in agreement with recently published λ_{max} values for "normal" macaque pigments.

Spectral Bandwidth of the α-Bands

As described in the Methods, the width of the α-band in each spectrum was determined in two segments, giving rise to three parameters. The data for the determination of means were taken from the same entries of Tables II–V as those used in the λ_{max} analysis. The corresponding parameter samples were pooled under the assumption that they were drawn from the same parent population. The standard error was then calculated from the estimated population variance (which was established by pooling the sample variances), while the appropriate degrees of freedom and the t scores for the 95% level of certainty were observed. Whenever possible, the spectrum of the average provided the LWHDBW, SWHDBW, and THDBW values for the mean, while the standard deviations were taken from the individually processed spectra. The individually processed mean SWHDBW and THDBW had to be used in those cases in which the average spectrum lacked these values because of high shortwave absorbance.

The mean LWHDBW, SWHDBW, and THDBW values obtained for the four visual pigments in cynomolgus are plotted in Fig. 7. The abscissa is $(\lambda_{max})^{-1}$ and the ordinate is bandwidth; both are measured in wavenumbers per centimeter. The solid lines were determined by regression analysis. The sides of each rectangle centered on a datum point correspond to the standard error at the 95% confidence level for the variables. The slope, y-intercept (i.e., the width at zero peak wavenumber), and correlation coefficient for the LWHDBW are 0.06746, 333 cm^{-1}, and 0.99129, respectively. Similarly, the characteristics in the same order for the THDBW are 0.06049, 2,834 cm^{-1}, and 0.93108. The SWHDBW regression line, having nearly zero slope and a small correlation coefficient, indicates a poor fit of data to the line. The most significant feature in Fig. 7 is the small scatter and good predictability of the LWHDBW as a function of $(\lambda_{max})^{-1}$. The THDBW appears to be a somewhat inferior predictor.

The bandwidths of macaque visual pigment spectra have been reported to have linear variation with peak wavenumber (or peak frequency) by Bowmaker et al. (1980), MacNichol et al. (1983), and Mansfield (1985). The functional dependence shown in Fig. 7 is in qualitative agreement with those results. However, the slope of the THDBW regression line found here is less steep than those that were published previously.

An unexpected feature in the plot of Fig. 7 is the apparent lack of frequency dependence of the SWHDBW. Although caution is advisable in drawing any

conclusion from the least reliable of the bandwidth parameters, the flatness of the SWHDBW may be relevant to Mansfield's idea. Mansfield (1985) proposed to scale the α-band portions of visual pigment absorbance spectra along both axes by plotting A/A_{max} vs. F/F_{max}. When the four macaque pigment spectra were scaled this way, he found near-coincidence of the longwave limbs, but the shortwave limbs diverged. His findings are in harmony with the regression lines reported here. On the basis of Fig. 7, one might suggest that the LWHDBW would be the best parameter to use in a Mansfield-type scaling because of its good linearity and its small y-intercept value. The THDBW regression line, however, is not suggestive of an invariant shape for the entire α-band.
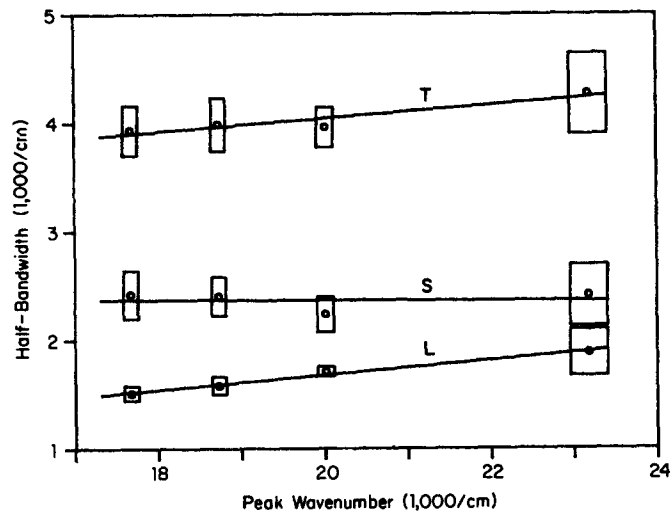
FIGURE 7. The variation of bandwidth vs. $(\lambda_{max})^{-1}$ of the four cynomolgus visual pigments. The bandwidth components of the α-bands (circles) are plotted separately; their regression lines are designated L (LWHDBW), S (SWHDBW), and T (THDBW). The sides of the rectangles about each point correspond to the standard error of the mean at the 95% confidence interval.

Specific Pigment Densities

The response of a photoreceptor depends on the light-catching ability of its pigment. The in vivo probability of capturing photons by a rod or cone cell is proportional to the total absorbance of the outer segment, i.e., the pathlength multiplied by the axial specific absorbance. Ideally, the specific pigment density should be determined axially, which is the physiological direction. For practical reasons, however, cells in vitro are measured mainly from the side. The reason this is acceptable is that, provided the light is polarized across the cell, the electric field intensity vector can be made to coincide with the direction that prevails under physiological conditions. Therefore, the absorbance measured transversely with light polarized perpendicular to the cell axis, $A_\perp$, is a quantity we need to know. When the peak $A_\perp$ is divided by the pathlength, often assumed to be equal to the cell's diameter, d, the transverse specific density, $D_\perp$, is obtained. It is easy

to show that $A_\perp$ is calculable from the average (unpolarized) transverse absorbance, A, and the dichroic ratio, R, as $A_\perp = A(2R)/(1 + R)$.

In the case of rods, which often maintain their geometrical form and linear dichroism for many hours postmortem, $D_\perp$ can be derived quite accurately. For example, the best cynomolgus super-rod measurement in this work resulted in A = 0.03179 at 500.8 nm and R = 3.77. From these, $A_\perp$ = 0.05029 is obtained using the formula above. The diameter of the outer segment was photographically determined (cf. Fig. 1) to be 3.0 μm ($\pm$10%), so that the specific density for natural light is $D = A/d$ = 0.0106 μm^{-1}, and that for transversely polarized light is $D_\perp = A_\perp/d$ = 0.0168 μm^{-1}. The latter value is high, and it approaches the highest transverse specific densities obtained from amphibian rods (e.g., Hárosi, 1975b). In contrast, when four cynomolgus super rods were averaged to yield A = 0.03148 and R = 2.68, then $A_\perp$ = 0.04585 was computed. However, given the lack of accurate information on cell dimensions, the specific density can only be estimated, e.g., $D_\perp$ = 0.04585/2.5 = 0.0183 μm^{-1}. The problem is similar with the common rods. Using A = 0.01228 for the average absorbance (Fig. 2A, trace a) and R = 3.28, the result was $A_\perp$ = 0.0188. The assumption of 1.0 μm for the average cell diameter would yield the high value of 0.0188 μm^{-1}; however, d = 1.5 μm would give 0.0125 μm^{-1}, which is probably too low.

Having inadequate information is an even greater problem in the case of cones. The rapid breakdown of their outer segments causes the loss of geometric form, precluding an accurate determination of both linear dichroism and pathlength. In order to provide a rudimentary approximation for the specific densities of cynomolgus blue, green, and red cones, Figs. 4A, 5A, and 6A were used, and their respective peak absorbances were determined. The missing information was assumed to be: average pathlength, 2.5 μm; average dichroic ratio, 3.0. Following the procedure outlined above, the average transverse specific densities were calculated for the three cone types. They were 0.0107, 0.0167, and 0.0142 μm^{-1}, respectively. Although these values should be regarded as no more than estimates, they compare favorably with those obtained by Bowmaker et al. (1978, 1980) and MacNichol et al. (1983).

Media for Cell Suspension

As described in the Methods, various media were used for the dissection and mounting of retinal tissue. Unfortunately, there were too many uncontrolled variables and too few experiments to enable one to draw definite conclusions. The use of taurine in a suspending medium (B$_2$, Table I) resulted in a successful experiment. However, subsequent applications of taurine did not consistently prove to protect primate cones from deterioration. Taurine also reacted with 11-cis-retinal in regeneration media, so its use was discontinued. Diamox, a carbonic anhydrase inhibitor, was also found to react with 11-cis-retinal, causing its abandonment. Although no dramatic improvement was observed with the inclusion of any one ingredient in the suspending and mounting media, the addition of 11-cis-retinal proved useful. It was found that although only ~30% of the preparations contained this supplement, >70% of the good BD spectra were derived from them. Thus, the clear-cut conclusion is that the use of

exogenous 11-cis-retinal, in addition to any other role it may play, can improve BD spectrum determinations.

Relevance to Human Vision

Old World primates have traditionally been grouped together as having very similar, if not identical, visual systems. De Valois et al. (1974) have examined this question perhaps the most carefully to date. They carried out extensive psychophysical testing of macaques and humans, and found that macaque monkeys (especially *M. fascicularis*) and normal human observers have the same flicker frequency response and Purkinje shift, and are very similar in both relative and absolute scotopic and photopic sensitivity. De Valois et al. argued that the great similarity between the hue and saturation discrimination functions for the macaque and normal human trichromats implies similarities not only in cone absorbance spectra, but also in the neural organization of their visual systems. The early microspectrophotometric experiments also supported this idea.

The homogeneity of visual pigments among the Old World primates has been questioned by Dartnall and co-workers. These researchers have carried out microspectrophotometric measurements on human photoreceptors, and obtained λ_{max} values that differed from the macaques' (Bowmaker and Dartnall, 1980; Dartnall et al., 1983a, b; Bowmaker et al., 1983). The most deviant λ_{max} of 419 ± 3.6 nm was derived from the blue-absorbing cones (Dartnall et al., 1983b). This value, if confirmed, would indeed violate the homogeneity of visual pigment absorbance spectra among the Old World primates. Supporting this idea, however, are the determinations by MacNichol et al. (1983) and Mansfield et al. (1984) on the rhesus and cynomolgus monkeys, by Bowmaker et al. (1983) on the baboon, whose blue cone λ_{max} was determined to be 432.5 ± 1.7 nm, and this contribution.

REFERENCES

Bevington, P. R. 1969. Data Reduction and Error Analysis for the Physical Sciences. McGraw-Hill Book Co., New York.

Bowmaker, J. K., and H. J. A. Dartnall. 1980. Visual pigments of rods and cones in a human retina. *Journal of Physiology.* 298:501–511.

Bowmaker, J. K., H. J. A. Dartnall, J. N. Lythgoe, and J. D. Mollon. 1978. The visual pigments of rods and cones in the rhesus monkey, *Macaca mulatta. Journal of Physiology.* 274:329–348.

Bowmaker, J. K., H. J. A. Dartnall, and J. D. Mollon. 1980. Microspectrophotometric demonstration of four classes of photoreceptors in an old world primate, *Macaca fascicularis. Journal of Physiology.* 298:131–143.

Bowmaker, J. K., J. D. Mollon, and G. H. Jacobs. 1983. Microspectrophotometric results for old and new world primates. *In* Colour Vision: Physiology and Psychophysics. J. D. Mollon and L. T. Sharpe, editors. Academic Press, Inc., London. 57–68.

Brown, P. K., and G. Wald. 1964. Visual pigments in single rods and cones of the human retina. *Science.* 144:45–51.

Bush, C. A. 1974. Fourier method for digital data smoothing in circular dichroism spectroscopy. *Analytical Chemistry.* 46:890–895.

Dartnall, H. J. A., J. K. Bowmaker, and J. D. Mollon. 1983a. Human visual pigments: microspectrophotometric results from the eyes of seven persons. *Proceedings of the Royal Society of London, Series B.* 220:115–130.

Dartnall, H. J. A., J. K. Bowmaker, and J. D. Mollon. 1983b. Microspectrophotometry of human photoreceptors. *In* Colour Vision: Physiology and Psychophysics. J. D. Mollon and L. T. Sharpe, editors. Academic Press, Inc., London. 69–80.

De Valois, R. L., H. C. Morgan, M. C. Polson, W. R. Mead, and E. M. Hull. 1974. Psychophysical studies of monkey vision. I. Macaque luminosity and color vision tests. *Vision Research.* 14:53–67.

Dobelle, W. H., W. B. Marks, and E. F. MacNichol, Jr. 1969. Visual pigment density in single primate foveal cones. *Science.* 166:1508–1510.

Goode, D. H., and M. Buchanan. 1980. A direct reading linear dichroism apparatus for extended wavelength ranges. *Review of Scientific Instruments.* 51:1121–1122.

Hárosi, F. I. 1975a. Microspectrophotometry: the technique and some of its pitfalls. *In* Vision in Fishes: New Approaches in Research. M. A. Ali, editor. Plenum Publishing Corp., New York. 43–54.

Hárosi, F. I. 1975b. Absorption spectra and linear dichroism of some amphibian photoreceptors. *Journal of General Physiology.* 66:357–382.

Hárosi, F. I. 1976. Spectral relations of cone pigments in goldfish. *Journal of General Physiology.* 68:65–80.

Hárosi, F. I. 1982a. Recent results from single-cell microspectrophotometry: Cone pigments in frog, fish and monkey. *Color Research and Application.* 7(Pt. 2, No. 2):135–141.

Hárosi, F. I. 1982b. Phase-modulated microspectrophotometry of photoreceptors. *Investigative Ophthalmology and Visual Science Supplement.* 22(3):189.

Hárosi, F. I. 1984. In vitro regeneration of visual pigment in isolated vertebrate photoreceptors. *In* Photoreceptors. A. Borsellino and L. Cervetto, editors. Plenum Publishing Corp., New York. 41–63.

Hárosi, F. I., and Y. Hashimoto. 1983. Ultraviolet visual pigment in a vertebrate: a tetrachromatic cone system in the dace. *Science.* 222:1021–1023.

Hárosi, F. I., and E. F. MacNichol, Jr. 1974a. Visual pigments of goldfish cones. Spectral properties and dichroism. *Journal of General Physiology.* 63:279–304.

Hárosi, F. I., and E. F. MacNichol, Jr. 1974b. Dichroic microspectrophotometer: a computer-assisted, rapid, wavelength-scanning photometer for measuring linear dichroism in single cells. *Journal of the Optical Society of America.* 64:903–918.

Jasperson, S. N., and S. E. Schnatterly. 1969. An improved method for high reflectivity

ellipsometry based on a new polarization modulation technique. *Review of Scientific Instruments.* 40:761–767.

Land, E. H., and C. D. West. 1946. Dichroism and dichroic polarizers. *In* Colloid Chemistry. J. Alexander, editor. Van Nostrand Reinhold Co., New York. 160–190.

Levine, J. S., and E. F. MacNichol, Jr. 1985. Microspectrophotometry of primate photoreceptors: art, artifact, and analysis. *In* The Visual System. A. Fein and J. S. Levine, editors. Alan R. Liss, Inc., New York. 73–87.

MacNichol, E. F., Jr. 1964. Retinal mechanisms of color vision. *Vision Research.* 4:119–133.

MacNichol, E. F., Jr. 1986. A unifying presentation of photopigment spectra. *Vision Research.* 26:1543–1556.

MacNichol, E. F. Jr., R. Feinberg, and F. I. Hárosi. 1973. Colour discrimination processes in the retina. *In* Colour 73. Proceedings for the Second Congress of the International Colour Association. Adam Hilger, Rank Precision Industries, Ltd., London. 191–251.

MacNichol, E. F., Jr., J. S. Levine, R. J. W. Mansfield, L. E. Lipetz, and B. A. Collins. 1983. Microspectrophotometry of visual pigments in primate photoreceptors. *In* Colour Vision: Physiology and Psychophysics. J. D. Mollon and L. T. Sharpe, editors. Academic Press, Inc., London. 13–38.

Mansfield, R. J. W. 1985. Primate photopigments and cone mechanisms. *In* The Visual System. A. Fein and J. S. Levine, editors. Alan R. Liss, Inc., New York. 89–106.

Mansfield, R. J. W., J. S. Levine, L. E. Lipetz, B. A. Collins, G. Raymond, and E. F. MacNichol, Jr. 1984. Blue-sensitive cones in the primate retina: microspectrophotometry of the visual pigment. *Experimental Brain Research.* 56:389–394.

Marks, W. B., W. H. Dobelle, and E. F. MacNichol, Jr. 1964. Visual pigments of single primate cones. *Science.* 143:1181–1183.

Robinson, E. A. 1967. Multichannel Time Series Analysis with Digital Computer Programs. Holden Day, San Francisco. 63–64.

Shapiro, S. S., and M. B. Wilk. 1965. An analysis of variance test for normality (complete samples). *Biometrika.* 52:591–611.

Treu, J. I., A. B. Collender, and S. E. Schnatterly. 1973. Use of a stable polarization modulation in a scanning spectrophotometer and ellipsometer. *Review of Scientific Instruments.* 44:793–797.